

AD-A046 074

LIGHTNING AND TRANSIENTS RESEARCH INST ST PAUL MN
INTEGRAL FUEL TANK SKIN MATERIAL HEATING FROM SWEPT SIMULATED L--ETC(U)
APR 77 J D ROBB, T CHEN
L/T-636

F/G 1/3

N00421-76-C-0052

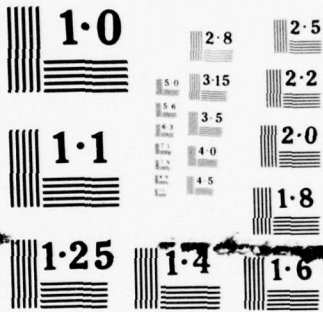
NL

UNCLASSIFIED

| OF |
ADA
046074



END
DATE
FILMED
11-77
DDC



NATIONAL BUREAU OF STANDARDS
MICROCOPY RESOLUTION TEST CHART

AD A 046074



INTEGRAL FUEL TANK SKIN MATERIAL HEATING

FROM

SWEPT SIMULATED LIGHTNING DISCHARGES

APRIL 1977

FOR

NAVAL AIR STATION

PATUXENT RIVER, MARYLAND 20670

CONTRACT NO. N00421-76-C-0052

BY

LIGHTNING AND TRANSIENTS RESEARCH INSTITUTE

ST. PAUL, MINN. 55113

DDC
RECEIVED
OCT 28 1977
A

AD No. _____
DDC FILE COPY

DISTRIBUTION STATEMENT A
Approved for public release;
Distribution Unlimited

6
AN EXPERIMENTAL STUDY
of
INTEGRAL FUEL TANK SKIN MATERIAL HEATING
from
SWEPT SIMULATED LIGHTNING DISCHARGES.

LIT Report No. 636

10 BY
J.D./Robb
T./Chen

14 L/P-636

11 April 1977

12 43p.

Prepared For

Naval Air Station
Patuxent River, Maryland 20670

Contract No. N00421-76-C-0052 *new*

15

Prepared By

Lightning & Transients Research Institute
2531 West Summer Street
St. Paul, Mn. 55113

9 Final rept.

DISTRIBUTION STATEMENT A
Approved for public release;
Distribution Unlimited

207350

207 350 1B

FOREWORD

This report, L&T No. 636, is the final report under Contract N00421-76-C-0052 with the Patuxent River Naval Air Test Center.

The researches were carried out by J.D. Robb and Dr. T. Chen with major assistance from Wm. Walker of Patuxent River Naval Air Test Center who was also the technical representative for the Patuxent River Naval Air Station.

NO. 636	NO.
DATE	Write Section <input checked="" type="checkbox"/>
DOC	Ref Section <input type="checkbox"/>
SPREADSHEET	<input type="checkbox"/>
BY <i>Per Form 50</i>	
DISTRIBUTION/AVAILABILITY CODES	
Dist.	AVAIL. and/or SPECIAL
<i>A</i>	

ABSTRACT

Studies have been carried out to determine the hot spot temperatures of swept laboratory lightning discharges using an infra red scanning camera, modified to provide higher time resolution with the LTRI St. Paul wind tunnel used to sweep the stroke. The data was compared with non swept (stationary arc) data. Somewhat higher energies were used in the test discharges corresponding to the new waveforms (SAE-Task F) including a 100,000 restrike and a 15 coulomb intermediate component superimposed on two hundred amperes of continuing current typical of natural lightning. The results indicate that with the thinner new materials, a hot spot ignition hazard definitely exists for the lower conductivity materials, titanium and stainless steel but less than had been previously estimated. Yet to be determined is the complete envelope of hot spot time duration versus temperature required for ignition.

1.0 INTRODUCTION AND SUMMARY

One of the areas of an aircraft most inherently vulnerable to lightning strikes is the fuel system and much effort has been directed over a period of many years to assure the safety of new systems through severe test standards. With the development of advanced aircraft having new and thinner skin materials, the question of possible heating of integral fuel tank skins to the spontaneous ignition temperature of the fuel becomes of renewed interest.

A number of earlier experimental studies using only stationary test discharges (without windstream) have indicated that aluminum could probably not cause hot spot ignition because of its excellent thermal and electrical conductivity unless puncture occurred and this was confirmed by theoretical studies. Of concern, however, are the newer materials including titanium and stainless steel with their much lower thermal and electrical conductivities.

The studies were carried out using an infra red scanning camera, modified to provide higher time resolution and with the LTRI St. Paul wind tunnel used to sweep the stroke. The data was compared with non swept (stationary arc) data. Somewhat higher energies were used in the test discharges corresponding to the new waveforms (SAE-Task F)* including a 100,000 restrike and a 15 coulomb intermediate component superimposed on two hundred amperes of continuing current typical of natural lightning. The results indicate that with the thinner new materials, a hot spot ignition hazard definitely exists for the lower conductivity materials, titanium and stainless steel but less than had been previously estimated. Yet to be determined is the complete envelope of hot spot time duration versus temperature required for ignition.

2.0 STROKE HEATING AND CONTACT MECHANISMS

Lightning stroke contact with integral fuel tank skins is established only in swept strike zones where the lightning sweeps over the skin as fuel tanks are not or should not be located in direct strike zones. The mechanisms of stroke contact heating are complex, involving plasma contact with the skin materials, ion bombardment and ohmic heating of the skin modified by heat transfer with phase change and windstream cooling.

Earlier researches have determined the charge transfer magnitudes as a function of the time required for puncture and also required for hot spot ignition using stationary (non swept) arcs (1,2,3). The minimum energy and charge transfers occurred at discharge times of about 10 to 20 milliseconds. These earlier researches had also shown typical stroke hang-on times of two to five milliseconds for titanium and aluminum respectively and even shorter times for stainless steel (4).

This data along with earlier theoretical and experimental studies of time temperature profiles (5) have indicated that without puncture, hot spot ignition with aluminum fuel tank skins is of very low probability.

With the trend toward thinner skins and the newer materials, the question of hot spot ignition again becomes of increased interest and an experimental program has been carried out to determine the time temperature waveforms.

3.0 EXPERIMENTAL ARRANGEMENT

The simulated lightning discharge arcs were swept over the test sample using a wind tunnel with the test sample held in a constant cross section throat area as shown in Figure 1. A Barnes infra red camera was located in an aluminum cabinet to provide shielding for the electronics with an opening only for the infra red optical path. Four artificial lightning generators were used to supply the initial continuing current and the combined high current and intermediate current restrike. The restrike was triggered by a high current rate of rise discharge from a separate generator. The waveform is shown in Figure 2 and a schematic diagram of the generators and their connections is shown in more detail in Figure 3.

Approximately three test runs were made for each test sample at each of three levels of charge transfer, 3, 9 and 15 coulombs. The maximum temperature recorded was taken as the measured value.

The test sample was masked with tape to provide a narrow test strip of bare metal along the direction of air flow and assure that the hot spots all fell within the narrow field of view of the infra red camera. To improve the time resolution, the Barnes infra red camera was used with the vertical scan disabled and with a narrow test sample. The IR scan was swept only along a narrow strip of the test sample at a rate of about 2 milliseconds per scan. The data was recorded on a Hewlett-Packard Type 3960C instrumentation tape recorder with a bandpass at 15 inches per second of 50 to 60,000 Hertz. The Barnes camera had a resolution of 10 milliradians equivalent to 120 kilohertz in the frequency domain but the tape recorder limited the resolution to about 20 milliradians (60 kilohertz) corresponding to about 5/8 inch of exposed width of test panel. The theoretical calculations indicated a backside temperature spot width at peak temperature of slightly less than 5/8th inch. Optical alignment of the camera with the test object, which was critical to the test result accuracy, was accomplished by placing a heated wire along the arc path and observing the Barnes output with an oscilloscope until the output was even along the entire scope trace.

The Barnes camera output was calibrated several times during the program using a laboratory standard "black body" temperature source with an appropriate aperture. The output was recorded on one channel of the tape recorder and a synchronization pulse was recorded on an adjacent channel.

The output had sufficient resolution to show clearly the temperature rise at major arc hang-on points as well as the spot width.

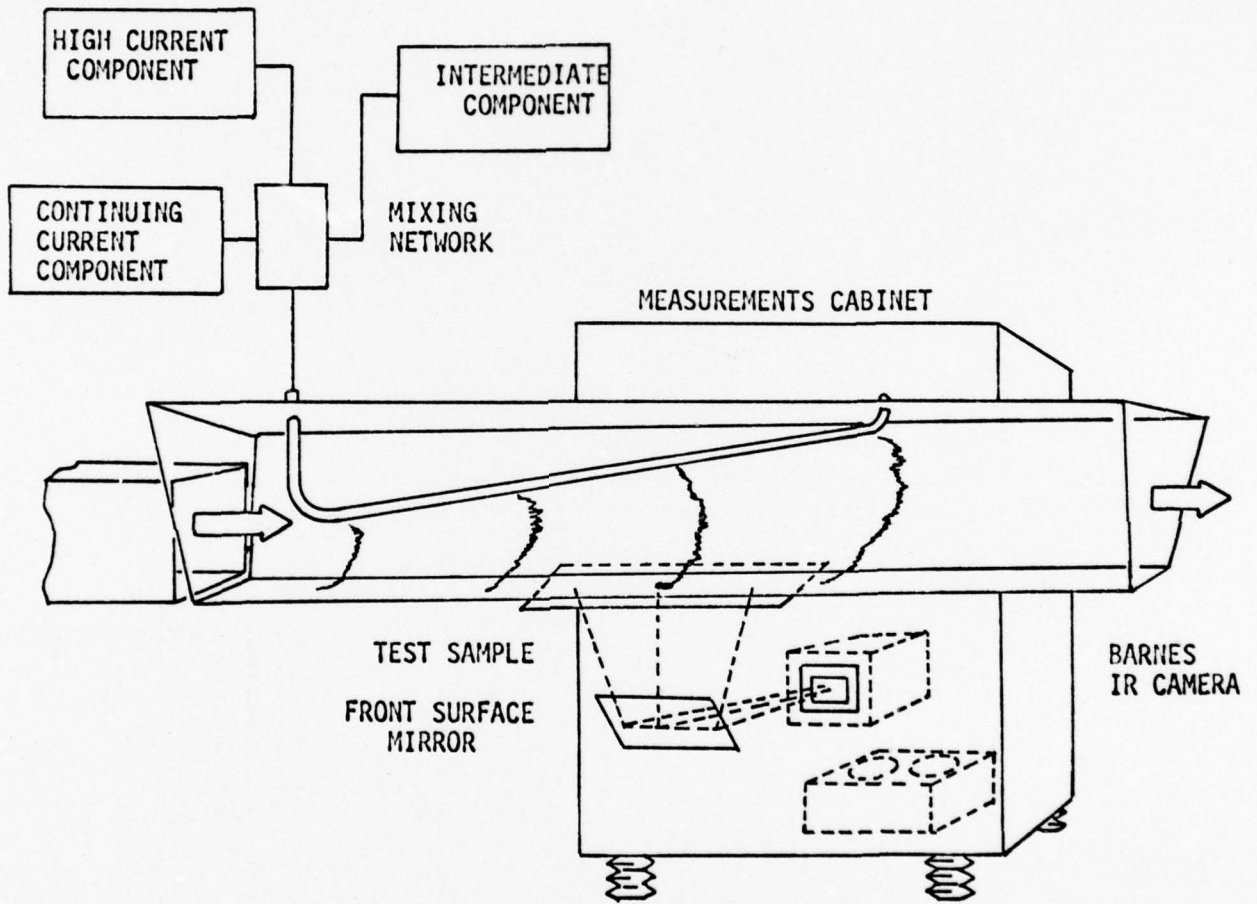


Figure 1. Test Arrangement for Swept Stroke Tests.

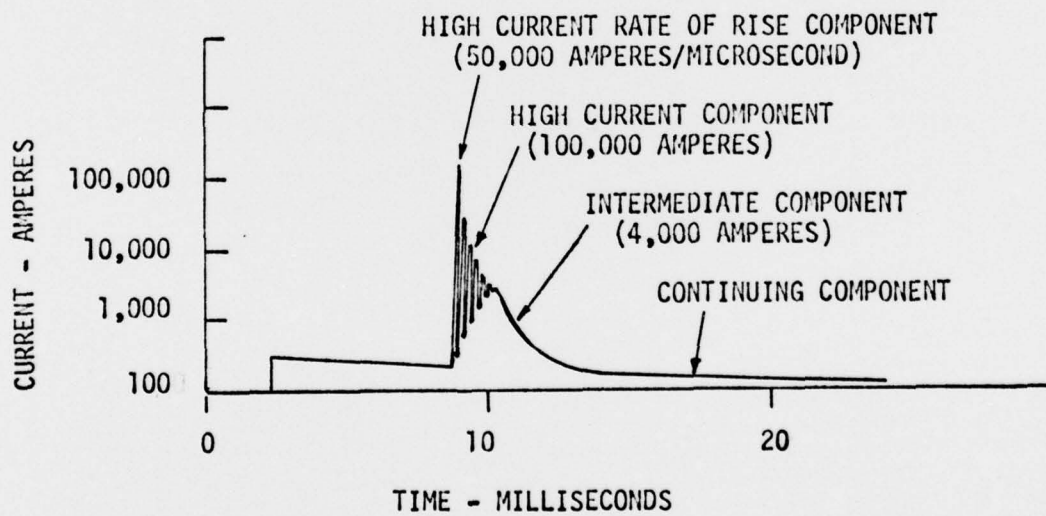


Figure 2. Test Current Waveform for Hot Spot Temperature Measurements.

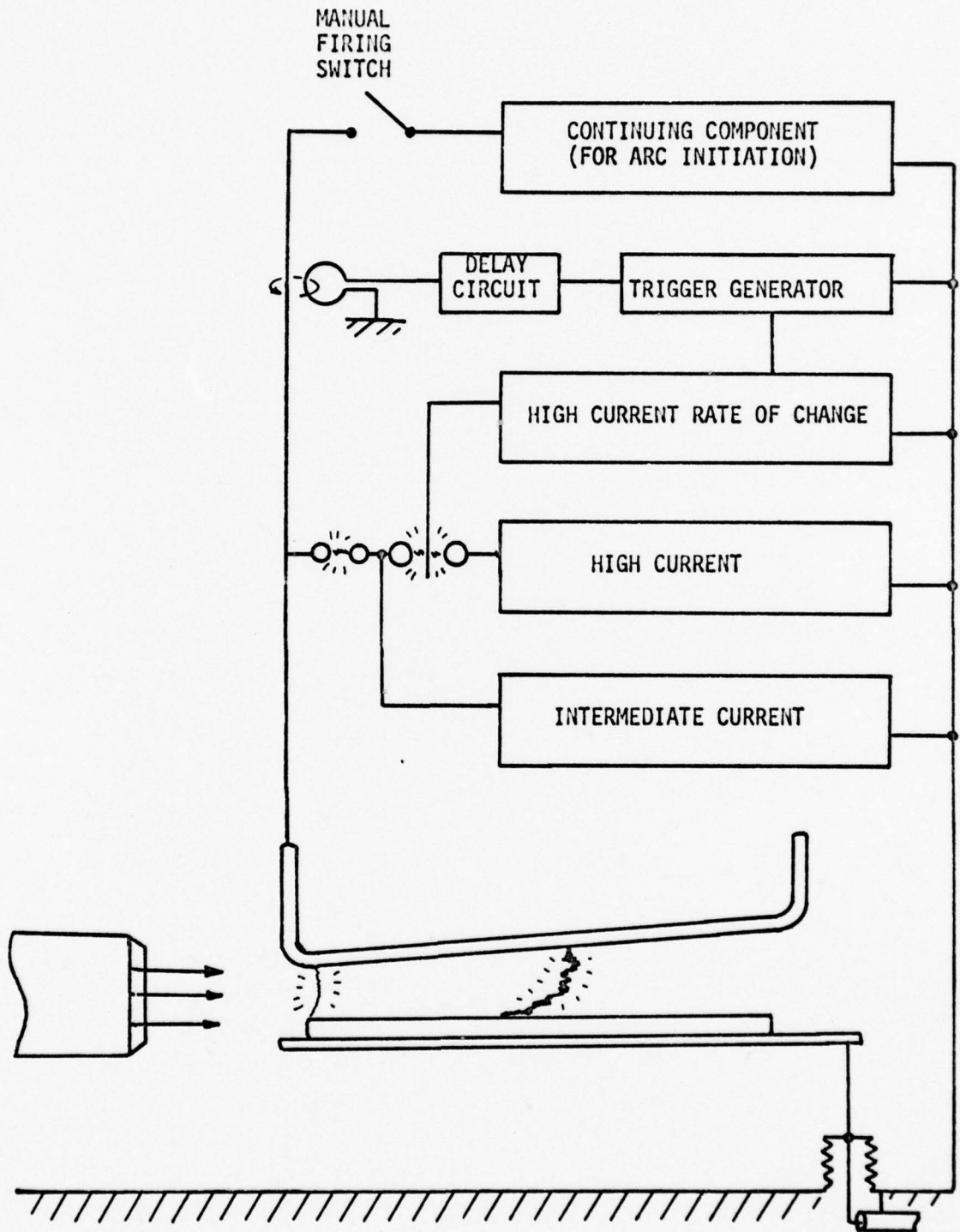


Figure 3. Multiple Generator Circuits Used for Generating High Energy in Hot Spot Studies.

4.0 ANALYSIS AND EXPERIMENTAL RESULTS

The theoretical analysis of the internal hot spot temperatures are complex because of the different heating modes; joule heating and ion bombardment and the phase changes - solid to liquid and liquid to vapor. In earlier LTRI theoretical studies (Appendix I and II), the hot spot time temperature profile of aluminum was calculated. In these calculations, a constant temperature heat input was assumed because of the thermal reservoir formed by a molten pool of aluminum and these calculations permit a comparison of the new materials coming into use for advanced aircraft. As illustrated in Figure 4 from L&T Report 333, the simplified calculation shows a faster rise and fall time and a lower peak temperature than was measured using a thermocouple with the stationary arc on aluminum. Apparently the molten metal slows the heat rise by holding the heat input at a temperature just above the melting temperature (659°C for aluminum) which is well below the arc temperature by at least an order of magnitude. The molten metal apparently also slows the temperature decay as it solidifies.

Tests were thus carried out using swept strokes on the new skin materials as outlined in Section 2. In the data reduction and analysis phase of the present program, the experimental results stored in the recording tape were reviewed in two basic forms, one in which the individual traces were shown as illustrated in Figure 5 to permit examination of the details of hang-on and temperature change and one in which only the envelope of the peak amplitudes were displayed for determining the peak temperature and, equally important, the rise and fall times as illustrated in Figure 6.

In Figure 5 are shown two hang-on points, one solid and one in which the arc is moving about considerably. Much higher temperatures are recorded for the point at which the arc is solidly attached as might be expected. Generally the point with the shortest total arc path length may be expected to hang the most solidly.

In Figure 6 are illustrated the great differences in rise and fall times and peak amplitudes for two different materials, aluminum above and stainless steel below. The much faster rise and fall times and lower amplitudes of the aluminum is illustrated. As the minimum ignition temperature is a function of the time duration, or in effect the total heat added, the much lower probability of fuel ignition with the aluminum is illustrated. This confirms the earlier experimental and theoretical studies of aluminum.

The wind tunnel tests have shown a great reduction in hot spot temperature with sweeping. A comparison between the swept and stationary arc (for a few metals run during the present program for direct comparison) show much lower temperatures by a factor of four to six and simple calculations do not indicate that simple windstream cooling of the skin would explain the difference. Greater evaporation of the molten metal and arc movement might. The measured values for the few samples in which both stationary and swept tests were made are presented in Table I.

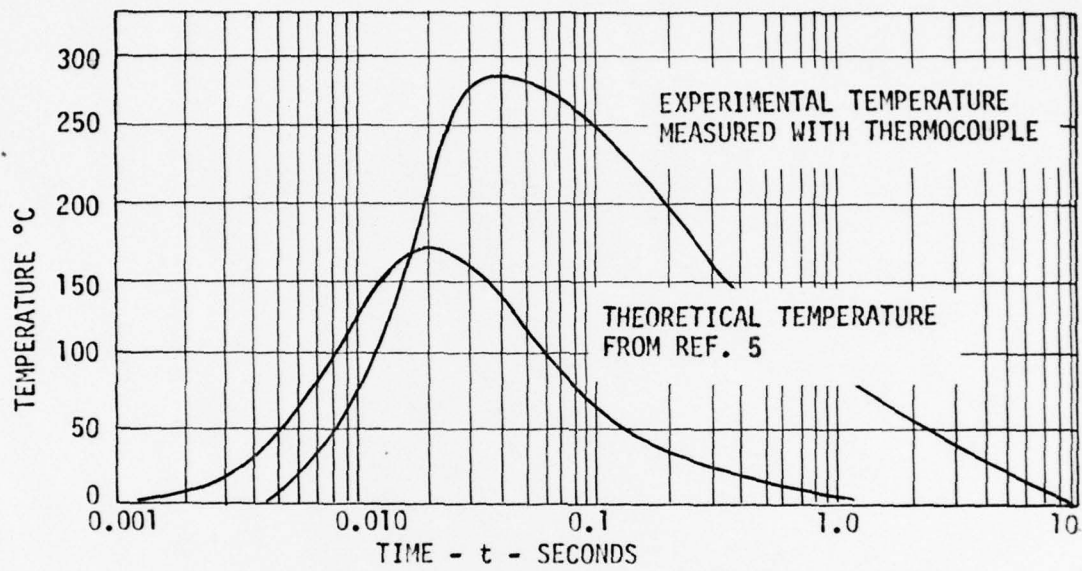


Figure 4. Experimental and Theoretical Time Temperature Curves for 1/8 inch Aluminum from Earlier Studies (5).

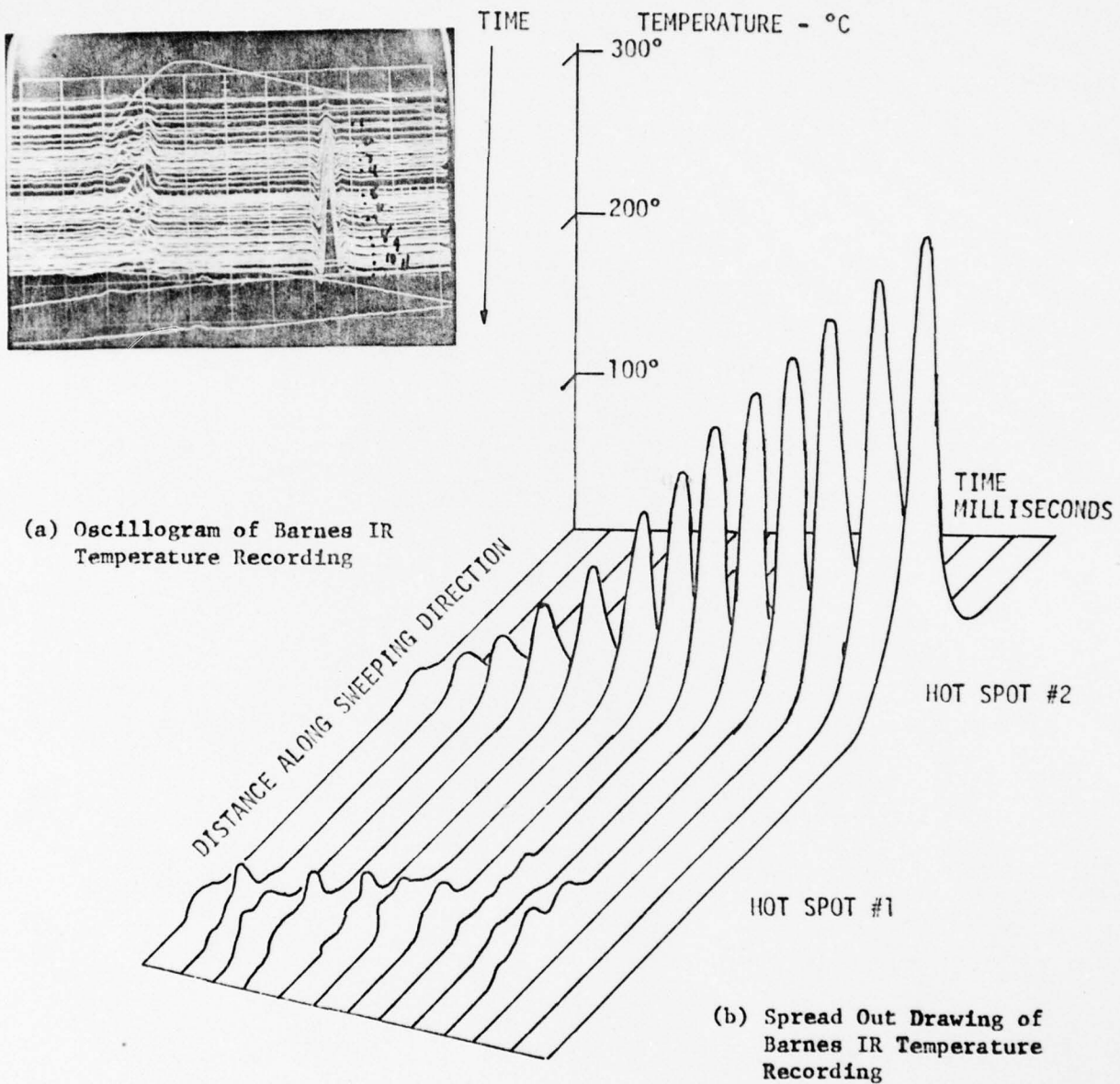
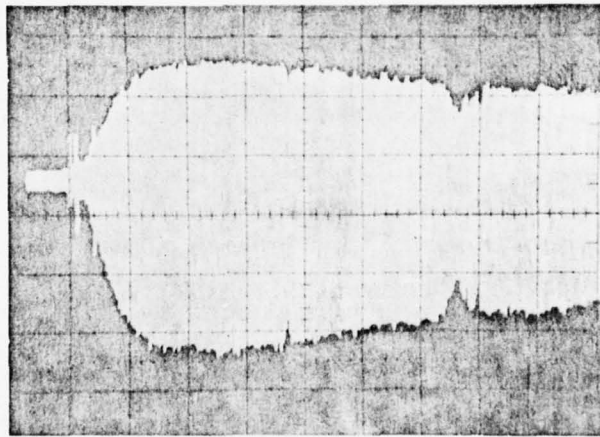
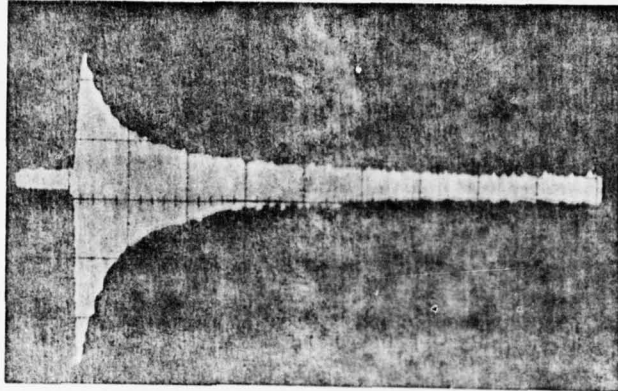


Figure 5. Time-Temperature Multiple Trace Plots Illustrate Typical Barnes Infra Red Display with Ordinate Used to Display Time.



HORIZONTAL SCALE - 0.125 SEC/DIV, VERTICAL - 314°C/ DIV

Figure 6. Oscillograms of Peak Temperature Envelopes Show Great Variation in Rise and Decay of 0.060 Aluminum (above) and Stainless Steel (below).

TABLE I

Hot Spot Metal Temperatures With Comparison of Swept and Stationary Arcs

	Aluminum t = 0.060	Titanium t = 0.090	Stainless Steel t = 0.060
Stationary	330°C	408°C	942°C
Swept	59°C	94°C	157°C
Ratio	5.6	4.3	6

A comparison of the temperatures between the LTRI theoretical calculations and the measured stationary and swept arcs using the infra red camera is shown in Figure 7. The figure illustrates that the swept stroke hot spot profiles lie well below the LTRI theoretical curves and much below the measured stationary arc temperatures.

A final summary of the temperatures as a function of restrike charge transfer is presented in Table II. As may be seen, with swept strokes, the boron and graphite have the highest temperatures followed by titanium and stainless steel in the middle range of thickness. It should again be emphasized that the hang-on times of the materials substantially affect the results, particularly the very low hang-on times of stainless steel which greatly reduces the relative hot spot temperature.

5.0 CONCLUSIONS AND RECOMMENDATIONS

Swept stroke temperatures from hot spot heating by lightning current arcs are substantially below the temperatures recorded with stationary arcs which have been used in all previous studies and on which most fuel ignition hazard evaluations have been made.

This data permits a major reevaluation of ignition hazards with the newer lower conductivity materials such as titanium and stainless steel. What remains to be determined, however, is the complete envelope of time temperature required for fuel vapor ignition and this is recommended for an additional study. This would permit determination of safety margins between the skin temperatures and the fuel vapor ignition time temperature profiles.

Also needing to be evaluated are the current time envelopes required for skin puncture with swept strokes and an evaluation of hot spot and puncture current time envelopes for painted skins. These are also recommended for an additional study as most aircraft now require painting for corrosion protection.

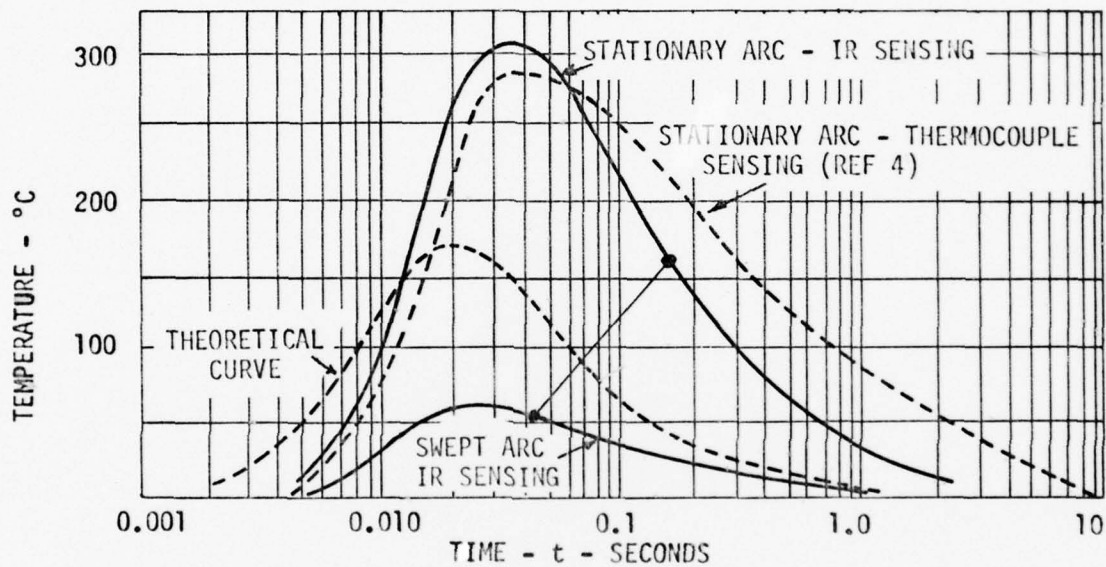


Figure 7. Measurements Show Greatly Reduced Hot Spot Temperatures with Swept Discharges.

TABLE II

Maximum Recorded Hot Spot Temperatures
With Corresponding Time Durations

<u>Test Sample</u>	<u>Temp. °C.</u>	<u>Time Duration - Seconds</u>
Aluminum 0.060 in.	59	0.218
Titanium 0.090	94	0.200
Stainless Steel 0.060	157	1.5

REFERENCES

1. Oh, L.L. and Schneider, S.D., "Lightning Strike Performance on Thin Metal Skin," Proceedings 1975 Lightning and Static Electricity Conference, 14 April 1975, Culham Laboratories, England.
2. Phillpott, J., "Factors Affecting Puncture of Aluminum Alloy by Simulated Lightning," Lightning and Static Electricity Conference, AFAL-TR-325, December 1972.
3. Walton, J.J. and Bootsma, P.H., "Measurement of Inner Skin Surface Temperatures of Aluminum Honeycomb Panels Subjected to Lightning Strikes," Proceedings 1975 Lightning and Static Electricity Conference, 14 April 1975, Culham Laboratories, England.
4. Robb, J.D. and Chen, T., "Theoretical Study of Fuel Tank Integral Skin Heating from Lightning Arc Contact," LTRI Report 638, April 1977.
5. Robb, J.D., Hill, E.L., Newman, M.M. and Stahmann, J.R., "Lightning Hazards to Aircraft Fuel Tanks," LTRI Report 333, September 1958.

APPENDIX I

L&T Report No. 638

April 1977

THEORETICAL STUDY OF
FUEL TANK INTEGRAL SKIN HEATING
FROM LIGHTNING ARC CONTACT

Period:	LTRI Industry Cooperative Program
Oct 76 - Mar 77	Lightning & Static Electrification Reduction

1.0 INTRODUCTION AND SUMMARY

Studies have been carried out to determine theoretical integral fuel tank skin temperatures when subjected to lightning swept stroke restrikes. The studies were made for the new fuel tank skin materials coming into use for advanced aircraft including titanium, stainless steel and graphite and boron epoxy. The new materials show much higher peak temperatures than aluminum used heretofore for nearly all integral fuel tank walls. The studies, along with current experimental measurements of fuel tank skin temperatures, permit a better evaluation of hot spot ignition hazards.

2.0 THEORETICAL BACKGROUND

The studies are based on earlier theoretical work (Appendix I) in the solution of the partial differential equation of heat flow for a quantity of heat at the melting temperature suddenly added to a finite volume in a thin plate. The basic assumption is that as long as the skin has not melted through to the inner surface that no puncture has occurred, the inner surface must remain below the melting temperature. The solution is carried out in rectangular coordinates for simplicity but could be converted to cylindrical coordinates which would not affect the results substantially. This solution does not recognize the complex mechanisms involved in the heat transfer process through joule heating and ion bombardment or in the phase changes from solid to liquid and liquid to vapor. These additional aspects considerably complicate the solutions and until they are better understood do not contribute significantly to greater confidence in the results than does the simple classical heat flow solution. The simpler solutions have

therefore been used to permit ready comparisons between the new materials. This data permits some interpolation of new experimental data on hot spot temperatures for both stationary and swept stroke arcs.

3.0 ANALYSIS

The results of the calculations are presented in Figures 1 through 4 and are presented in both log linear and linear coordinates. On each graph is also plotted an estimated minimum ignition time-temperature curve based on the few presently available data points with straight line interpolation between the extremities. The plots are presented for several materials of the same thickness to permit comparison of temperature profiles.

Of interest is the short duration of the temperature pulse of titanium. As the total time temperature integral determines the ignition probability, titanium would seem to be superior to stainless steel because of the more rapid temperature drop. It should be noted that in experimental studies, stainless steel has been shown to have, however, a very short hang-on time (Appendix II) which balances its longer duration hot spot.

In tests of 0.012" (12/1000) nickel plated stainless steel, no puncture occurred from 100,000 ampere discharges with intermediate currents between five and ten coulombs. This was attributed to the low hang on time and arc spread characteristics. There were about 100 pit marks per foot spread both laterally and longitudinally as shown in Appendix II. Incidentally it should be noted that the tubing was pressurized during the tests to 2650 psi. Boron and graphite, because of their much higher melting temperatures, show significantly higher hot spot temperatures than titanium and stainless steel.

From these calculations, an estimate of the relative capacities of the various materials to withstand lightning discharge currents is shown. It should be noted that as with the stainless steel swept stroke tests of Appendix II, a critical factor is sweeping which greatly reduces the hot spot temperature. This is also indicated in Appendix III, a paper on some experimental measurements of inner skin temperatures with swept strokes.

4.0 CONCLUSIONS

Theoretical studies of fuel tank skin material hot spot temperatures caused by lightning restrike currents have shown the much higher temperatures reached by titanium and stainless steel, but also the much shorter duration of the titanium temperature pulse as compared to stainless steel. Even higher temperatures are indicated for boron and graphite epoxy.

ESTIMATED SPONTANEOUS
IGNITION TEMPERATURE

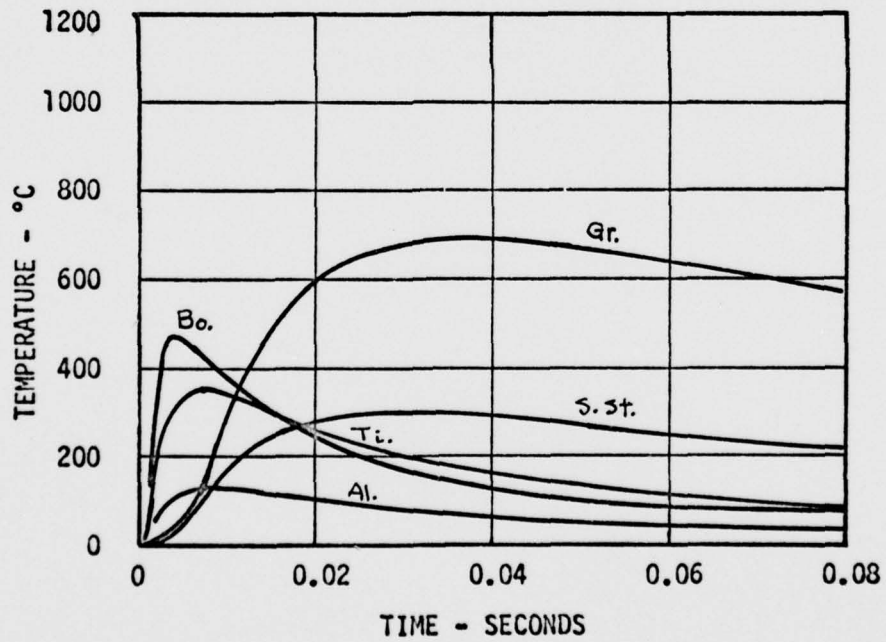
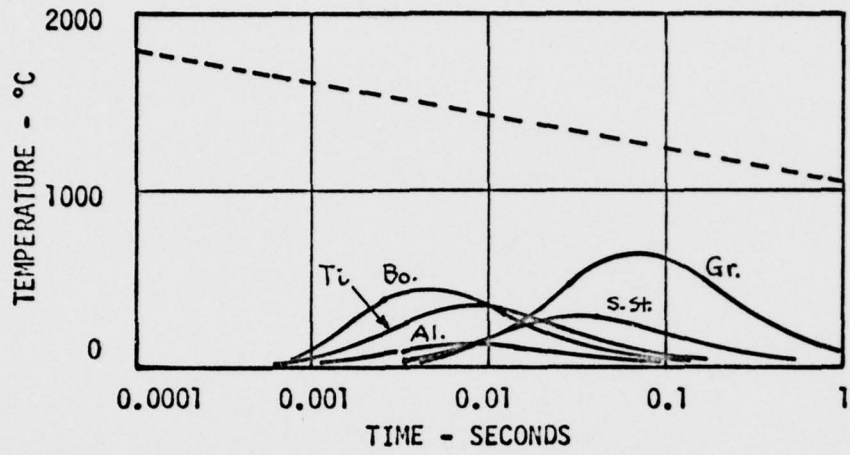


Figure 1. Calculated Hot Spot Temperature for Five Materials of 0.12 Thickness.

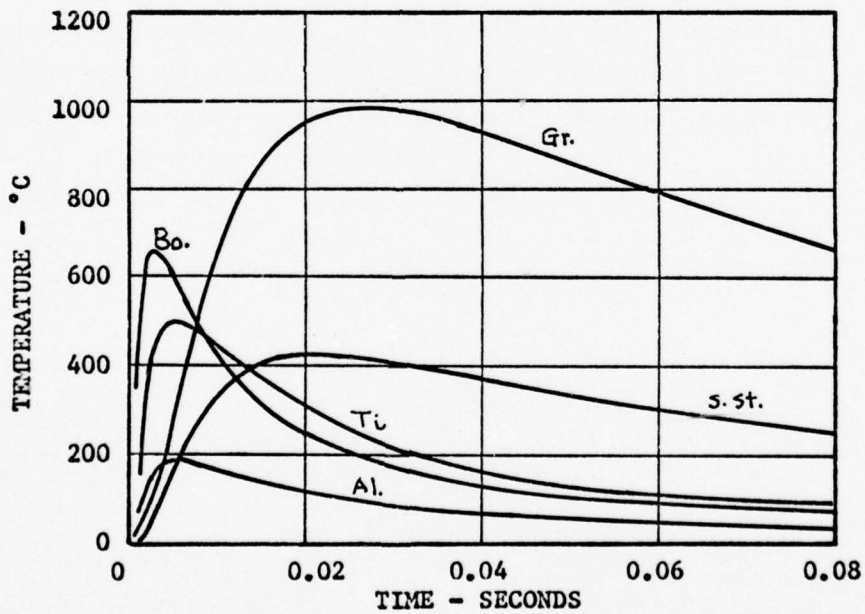
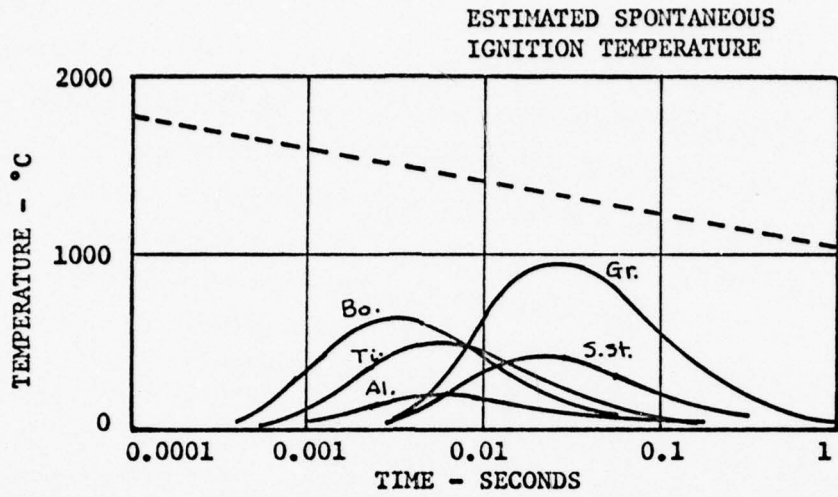


Figure 2. Calculated Hot Spot Temperature for Five Materials of 0.09 Inch Thickness.

ESTIMATED SPONTANEOUS
IGNITION TEMPERATURE

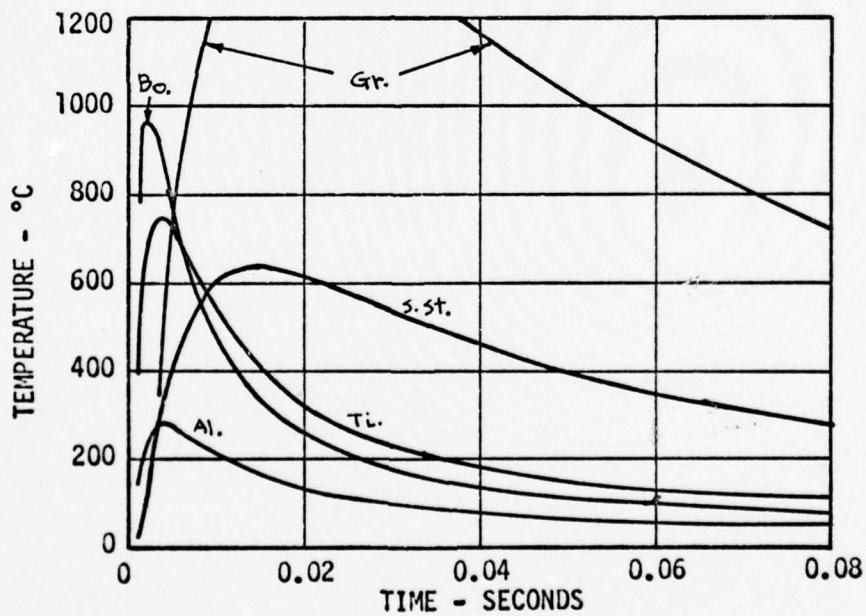
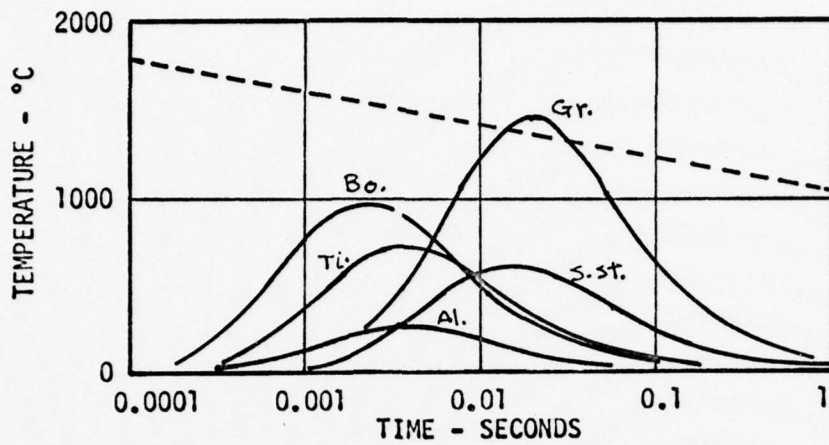


Figure 3. Calculated Hot Spot Temperature for Five Materials of 0.06 Inch Thickness.

ESTIMATED SPONTANEOUS
IGNITION TEMPERATURE

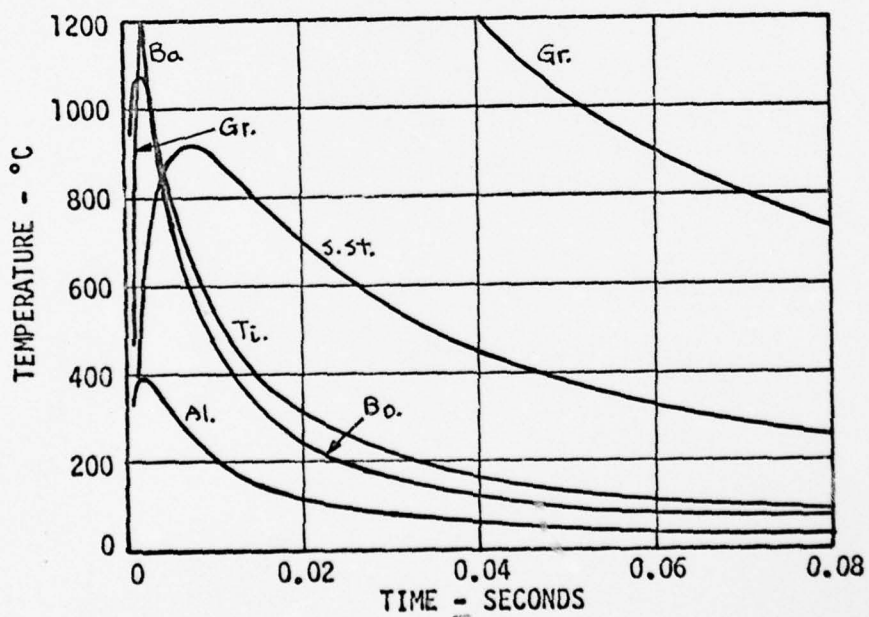
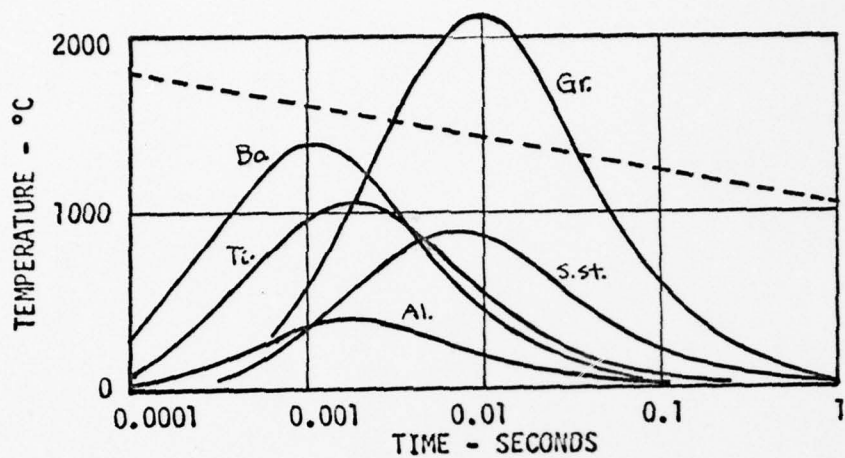


Figure 4. Calculated Hot Spot Temperature for Five Materials of 0.03 Inch Thickness.

APPENDIX II

Excerpt From LTRI Report 333

APPENDIX II

HEAT FLOW IN A PLATE DUE TO LIGHTNING STROKE

Introduction

When a lightning stroke hits a metal plate, such as a structural member of an airplane, it may burn through the plate or it may burn out only a small pool of metal, causing a pitting of the plate. Of course, the worst damage is caused when a hole is burned through the plate. The material on the back side is then open to damage by the arc; and, if a member such as a gas tank is involved, explosion may result.

Even if the plate is not burned through, there may be a sufficiently great release of heat energy in the plate to lead to severe damage. The question is whether a large enough temperature rise may occur on the inner surface of the wall of a gas tank to initiate an explosion in the tank. This problem in heat conduction is theoretically analyzed herein.

Theory

Consider a metal plate in the form of a square of side a and of thickness b , with $a \gg b$. Take a rectangular set of coordinate axes with origin at the center point of one side of the plate, referred to as the inside surface. Orient the x, y -axes parallel to the sides of the plate, and the z -axis normal to the inside surface. The outside surface of the plate then corresponds to the surface $z = b$. The lightning stroke will be supposed to strike the outside surface of the plate at the point $(0, 0, b)$, directly opposite the origin of coordinates O of the coordinate system, and to release there a quantity of heat Q at time $t = 0$. The problem is to evaluate the temperature distribution on the inner surface of the plate as a function of time; in particular, the temperature at the point O , which will be the hottest point on the inner surface.

Since this is a damage problem, it is best to set the conditions on the analysis so that the temperature rise on the inner surface will be overestimated rather than underestimated. Therefore, the analysis is simplified by supposing that no heat is lost from the plate either by radiation or by conduction to the air.

The heat-conduction equation

$$\left(\nabla^2 - \frac{\partial}{\partial t} \right) T = 0 \quad (1)$$

is to be solved in the region

$$\left. \begin{aligned} \frac{-a}{2} &\leq x \leq \frac{a}{2} \\ \frac{-a}{2} &\leq y \leq \frac{a}{2} \\ 0 &\leq z \leq b \end{aligned} \right\} \quad (2)$$

with the boundary conditions

$$\left. \begin{aligned} \frac{\partial T}{\partial x} &= 0 \quad \text{at} \quad x = \pm \frac{a}{2} \\ \frac{\partial T}{\partial y} &= 0 \quad \text{at} \quad y = \pm \frac{a}{2} \\ \frac{\partial T}{\partial z} &= 0 \quad \text{at} \quad z = 0, b \end{aligned} \right\} \quad (3)$$

The following functions are special solutions of the heat-conduction equation (1) that satisfy the boundary conditions (3):

$$\cos \left[\left(\frac{l\pi}{a} \right) \left(x + \frac{a}{2} \right) \right] \cos \left[\left(\frac{m\pi}{a} \right) \left(y + \frac{a}{2} \right) \right] \cos \left[\left(\frac{n\pi}{b} \right) z \right] \exp(-\lambda_{lmn}t) \quad (4)$$

where l , m , and n are non-negative integers and

$$\lambda_{lmn} = \pi^2 \left[\left(\frac{l\pi}{a} \right)^2 + \left(\frac{m\pi}{a} \right)^2 + \left(\frac{n\pi}{b} \right)^2 \right] \quad (5)$$

Next, these particular solutions are combined in such a manner that the initial conditions representing the heat source produced on the outside of the plate by the lightning stroke are satisfied. For this purpose the general solution for the temperature at any point in the plate is formed:

$$T(x, y, z, t) = \sum_{l, m, n=0}^{\infty} A_{lmn} \left\{ \cos \left[\left(\frac{l\pi}{a} \right) \left(x + \frac{a}{2} \right) \right] \cos \left[\left(\frac{m\pi}{a} \right) \left(y + \frac{a}{2} \right) \right] \cos \left[\left(\frac{n\pi}{b} \right) z \right] \exp(-\lambda_{lmn}t) \right\} \quad (6)$$

Let the temperature distribution at $t = 0$ be known, so that

$$T(x, y, z, 0) = u(x, y, z) \quad (7)$$

is a known function of the coordinates x, y, z in the plate. Combining equations (6) and (7) gives

$$u(x, y, z) = \sum_{l, m, n=0}^{\infty} A_{lmn} \left\{ \cos \left[\left(\frac{l\pi}{a} \right) \left(x + \frac{a}{2} \right) \right] \cos \left[\left(\frac{m\pi}{a} \right) \left(y + \frac{a}{2} \right) \right] \cos \left[\left(\frac{n\pi}{b} \right) z \right] \right\} \quad (8)$$

In order to express the coefficients in this Fourier series in terms of the function $u(x, y, z)$, the symbol $M[F(x, y, z)]$ is defined as the mean value of the function $F(x, y, z)$ over the volume of the plate. That is,

$$M[F(x, y, z)] = \frac{1}{a^2 b} \int_{-a/2}^{a/2} \int_{-a/2}^{a/2} \int_0^b F(x, y, z) dz dy dx \quad (9)$$

where $a^2 b$ is the volume of the plate.

Using equation (8) and the usual methods of calculating the coefficients in a Fourier series gives

$$A_{lmn} = \frac{M \left\{ u(x, y, z) \cos \left[\left(\frac{l\pi}{a} \right) \left(x + \frac{a}{2} \right) \right] \cos \left[\left(\frac{m\pi}{a} \right) \left(y + \frac{a}{2} \right) \right] \cos \left[\left(\frac{n\pi}{b} \right) z \right] \right\}}{M \left\{ \cos^2 \left[\left(\frac{l\pi}{a} \right) \left(x + \frac{a}{2} \right) \right] \cos^2 \left[\left(\frac{m\pi}{a} \right) \left(y + \frac{a}{2} \right) \right] \cos^2 \left[\left(\frac{n\pi}{b} \right) z \right] \right\}} \quad (10)$$

The evaluation of the initial temperature distribution $u(x, y, z)$ requires simulating the heating effect of the lightning stroke in some suitable fashion. Suppose that at $t = 0$ an amount of heat Q is liberated in a small block of the plate defined by the conditions

$$\left. \begin{aligned} \frac{-a}{2} < \frac{-\alpha}{2} \leq x \leq \frac{\alpha}{2} < \frac{a}{2} \\ \frac{-a}{2} < \frac{-\alpha}{2} \leq y \leq \frac{\alpha}{2} < \frac{a}{2} \\ b - \beta \leq z \leq b \end{aligned} \right\} \quad (11)$$

The heat is thus liberated in the small block of dimensions α, α, β situated on the outer surface of the plate, just opposite the point 0 on the plate. The material in this block will be raised to the uniform temperature

$$\theta = \frac{Q}{c\rho\alpha^2\beta} \quad (12)$$

where c is the specific heat and ρ is the density of the metal. The function $u(x, y, z)$ will be equal to θ in this block and equal to zero outside it.

The coefficients A_{lmn} from equation (10) can now be evaluated as follows:

$$A_{lmn} = \theta \frac{\left\{ \frac{1}{a} \int_{-a/2}^{a/2} \cos \left[\left(\frac{l\pi}{a} \right) \left(x + \frac{a}{2} \right) \right] dx \right\} \left\{ \frac{1}{a} \int_{-a/2}^{a/2} \cos \left[\left(\frac{m\pi}{a} \right) \left(y + \frac{a}{2} \right) \right] dy \right\} \left\{ \frac{1}{b} \int_{b-\beta}^b \cos \left[\left(\frac{n\pi}{b} \right) z \right] dz \right\}}{\left[\frac{1}{2}(1 + \delta_{l,0}) \right] \left[\frac{1}{2}(1 + \delta_{m,0}) \right] \left[\frac{1}{2}(1 + \delta_{n,0}) \right]} \quad (13)$$

For convenience of notation the Kronecker symbols are used:

$$\delta_{l,0} = \begin{cases} 1 & \text{if } l = 0 \\ 0 & \text{if } l \neq 0 \end{cases} \quad (14)$$

Carrying out the integrations indicated in equation (13) yields

$$\begin{aligned} \frac{1}{a} \int_{-a/2}^{a/2} \cos \left[\left(\frac{l\pi}{a} \right) \left(x + \frac{a}{2} \right) \right] dx &= \frac{1}{l\pi} \left\{ \sin \left[\left(\frac{l\pi}{a} \right) \left(\frac{a+a}{2} \right) \right] - \sin \left[\left(\frac{l\pi}{a} \right) \left(\frac{a-a}{2} \right) \right] \right\} \\ &= \left(\frac{2}{l\pi} \right) \sin \left(\frac{\alpha l\pi}{2a} \right) \cos \left(\frac{l\pi}{2} \right) \\ &= \begin{cases} 0 & \text{if } l \text{ is odd} \\ (-)^{l/2} \frac{\sin \left(\frac{l\pi\alpha}{2a} \right) \frac{\alpha}{a}}{\frac{l\pi\alpha}{2a}} & \text{if } l \text{ is even} \end{cases} \end{aligned} \quad (15)$$

$$\begin{aligned}
\frac{1}{b} \int_{b-\beta}^b \cos \left[\left(\frac{n\pi}{b} \right) z \right] dz &= \frac{1}{n\pi} \left\{ \sin(n\pi) - \sin \left[n\pi \left(\frac{b-\beta}{b} \right) \right] \right\} \\
&= \left(\frac{2}{n\pi} \right) \sin \left(\frac{n\pi\beta}{2b} \right) \cos \left[n\pi \left(\frac{2b-\beta}{2b} \right) \right] \\
&= (-)^n \left(\frac{2}{n\pi} \right) \sin \left(\frac{n\pi\beta}{2b} \right) \cos \left(\frac{n\pi\beta}{2b} \right) \\
&= (-)^n \left(\frac{\beta}{b} \right) \frac{\sin \left(\frac{n\pi\beta}{b} \right)}{\frac{n\pi\beta}{b}} \quad (16)
\end{aligned}$$

This yields the general formula

$$A_{lmn} = \theta \frac{\frac{\alpha^2\beta}{a^2b}}{\left[\frac{1}{2}(1+\delta_{l,0}) \right] \left[\frac{1}{2}(1+\delta_{m,0}) \right] \left[\frac{1}{2}(1+\delta_{n,0}) \right]} (-)^{[(l+m)/2]+n} \frac{\sin \left(\frac{l\pi\alpha}{2a} \right) \sin \left(\frac{m\pi\alpha}{2a} \right) \sin \left(\frac{n\pi\beta}{b} \right)}{\left(\frac{l\pi\alpha}{2a} \right) \left(\frac{m\pi\alpha}{2a} \right) \left(\frac{n\pi\beta}{b} \right)} \quad (17)$$

Here l and m have only even values, since by equation (15) the coefficient A_{lmn} will vanish if l or m is odd.

The final solution of equation (6) for the temperature distribution in the plate for $t \geq 0$ can be written as

$$T(x, y, z, t) = \frac{Q}{c\rho\alpha^2\beta} \varphi(a, \alpha; x, t) \varphi(a, \alpha; y, t) \psi(b, \beta; z, t) \quad (18)$$

where

$$\varphi(a, \alpha; x, t) = \sum_{l=0, 2, 4, \dots}^{\infty} \frac{(-)^{l/2} \frac{\alpha}{a} \cos \left[\left(\frac{l\pi}{a} \right) \left(x + \frac{a}{2} \right) \right]}{\frac{1}{2}(1 + \delta_{l,0})} \frac{\sin \left(\frac{l\pi\alpha}{2a} \right)}{\frac{l\pi\alpha}{2a}} \exp \left[- \left(\frac{l\pi\alpha}{a} \right)^2 t \right] \quad (19)$$

$$\psi(b, \beta; z, t) = \sum_{n=0, 1, 2, \dots}^{\infty} \frac{(-)^n \frac{\beta}{b} \cos \left[\left(\frac{n\pi}{b} \right) z \right]}{\frac{1}{2}(1 + \delta_{n,0})} \frac{\sin \left(\frac{n\pi\beta}{b} \right)}{\frac{n\pi\beta}{b}} \exp \left[- \left(\frac{n\pi\beta}{b} \right)^2 t \right] \quad (20)$$

If l is even,

$$\cos \left[\left(\frac{l\pi}{a} \right) \left(x + \frac{a}{2} \right) \right] = (-1)^{l/2} \cos \left(\frac{l\pi x}{a} \right) \quad (21)$$

so that the new summation index, $p = l/2$, can be introduced, which takes all non-negative integral values, and formula (19) can be replaced by

$$\varphi(a, \alpha; x, t) = \sum_{p=0,1,2,\dots}^{\infty} \frac{\frac{\alpha}{a} \cos \left(\frac{2p\pi x}{a} \right) \sin \left(\frac{p\pi \alpha}{a} \right)}{\frac{1}{2}(1 + \delta_{l,0}) \frac{p\pi \alpha}{a}} \exp \left[- \left(\frac{2p\pi x}{a} \right)^2 t \right] \quad (22)$$

The formulas given represent the exact solution of the proposed problem. However, in view of the nature of the applications to be made of them, it is feasible to allow some simplifications.

The size of the plate is not very material to the flow of the heat to the inside of the plate so long as the thickness is small compared with the breadth of the plate. It is therefore convenient to take the limit $a \rightarrow \infty$. In this case,

$$\varphi(\alpha; x, t) = \lim_{a \rightarrow \infty} \varphi(a, \alpha; x, t) \quad (23)$$

The series in equation (22) goes over into an integral, and on working out the process the following solution is found:

$$\varphi(\alpha; x, t) = \frac{2}{\pi} \int_0^{\infty} \frac{\sin \xi}{\xi} \cos \left(\frac{2x\xi}{a} \right) \exp \left[- \left(\frac{2x\xi}{a} \right)^2 t \right] d\xi \quad (24)$$

where $\xi = p\pi\alpha/a$.

This function can be reduced to a more convenient form for numerical computations. Introduce the following notation (which is valid for $t > 0$):

$$\left. \begin{aligned} \mu &= \left(\frac{2x\sqrt{t}}{a} \right) \xi \\ \xi &= \left(\frac{a}{2x\sqrt{t}} \right) \mu \end{aligned} \right\} \quad (25)$$

Substitution into equation (24) yields

$$\begin{aligned}\varphi(\alpha; x, t) &= \frac{2}{\pi} \int_0^{\infty} \frac{\sin\left(\frac{\alpha\mu}{2x\sqrt{t}}\right)}{\mu} \cos\left(\frac{x\mu}{x\sqrt{t}}\right) \exp(-\mu^2) d\mu \\ &= \frac{1}{\pi} \int_0^{\infty} \left[\sin\left(\frac{x + \frac{\alpha}{2x}}{x\sqrt{t}} \mu\right) - \sin\left(\frac{x - \frac{\alpha}{2x}}{x\sqrt{t}} \mu\right) \right] \frac{\exp(-\mu^2)}{\mu} d\mu\end{aligned}\quad (26)$$

Now define the function

$$g(\eta) = \frac{2}{\pi} \int_0^{\infty} \frac{\sin(2\eta\mu)}{\mu} \exp(-\mu^2) d\mu \quad (27)$$

Making use of this abbreviation gives from equation (26),

$$\varphi(\alpha; x, t) = \frac{1}{2} \left[g\left(\frac{x + \frac{\alpha}{2x}}{x\sqrt{t}}\right) - g\left(\frac{x - \frac{\alpha}{2x}}{x\sqrt{t}}\right) \right] \quad (28)$$

From equation (27),

$$\begin{aligned}\frac{dg}{d\eta} &= \frac{4}{\pi} \int_0^{\infty} \cos(2\eta\mu) \exp(-\mu^2) d\mu \\ &= \frac{2}{\sqrt{\pi}} \exp(-\eta^2)\end{aligned}\quad (29)$$

on making use of formula 508 of Peirce's table of integrals (ref. 2). It is obvious from equation (27) also that $g(0) = 0$. Equation (29) is integrated directly as a differential equation:

$$g(\eta) = \frac{2}{\sqrt{\pi}} \int_0^{\eta} \exp(-\mu^2) d\mu \quad (30)$$

This shows that the function $g(\eta)$ defined in equation (27) is just the ordinary probability integral and thus can be found tabulated in numerical form.

The following formula for the temperature distribution from the heat source (strictly speaking, in a plate of infinite breadth) is finally obtained:

$$T(x, y, z, t) = \frac{Q}{c\rho\alpha^2\beta} \varphi(\alpha; x, t)\varphi(\alpha; y, t)\psi(b, \beta; z, t) \quad (31)$$

with the function $\varphi(\alpha; x, t)$ defined by equation (28) and the function $\psi(b, \beta; z, t)$ defined by equation (20).

Discussion of Formula (31)

Formula (31) gives the temperature distribution throughout the plate resulting from the heat source introduced by the lightning stroke. In applying the result, only the temperature distribution over the inner surface needs to be known. This is obtained by setting $z = 0$ in equation (31). For simplicity of notation, this temperature function is written as follows:

$$T_0(x, y; t) = T(x, y, 0; t) \quad (32)$$

The following formula results:

$$T_0(x, y; t) = \frac{Q}{c\rho\alpha^2\beta} \varphi(\alpha; x, t)\varphi(\alpha; y, t)\psi(b, \beta; 0, t) \quad (33)$$

where, from equation (20),

$$\psi(b, \beta; 0, t) = \frac{\beta}{b} \sum_{n=0, 1, \dots}^{\infty} \frac{(-)^n \sin\left(\frac{n\pi\beta}{b}\right)}{\frac{1}{2}(1 + \delta_{n,0})\left(\frac{n\pi\beta}{b}\right)} \exp\left[-\left(\frac{n\pi\beta}{b}\right)^2 t\right] \quad (34)$$

Since the temperature distribution $T_0(x, y; t)$ is expressed in equation (33) as the product of two types of functions, it is convenient to examine the nature of each of these functions separately.

At the initial instant $t = 0$, conditions require that the whole of the inner surface of the plate be at the uniform temperature taken to be $T = 0$. Therefore, the following must be obtained from equation (34):

$$\psi(b, \beta; 0, 0) = \frac{\beta}{b} \sum_{n=0}^{\infty} \frac{(-)^n \sin\left(\frac{n\pi\beta}{b}\right)}{\frac{1}{2}(1 + \delta_{n,0})\left(\frac{n\pi\beta}{b}\right)} = 0 \quad (35)$$

This is an alternating series of a type somewhat difficult to handle, since the terms do not diminish very rapidly in magnitude. There will be no attempt to prove rigorously that the sum of the series is actually zero as is indicated in equation (35).

It is apparent by inspection of equation (34) that as $t \rightarrow \infty$ the series converges rapidly to the value

$$\psi(b, \beta; 0, \infty) = \frac{\beta}{b} \quad (36)$$

Owing to the exponential nature of the summands in the series in their dependence on the time variable, the dominating term will be the one having the smallest exponent; that is, the second member of the series, since the first one ($n = 0$) does not depend on the time at all. Therefore, the function given by equation (34) will start from zero at $t = 0$ and will rise quickly to the final value β/b practically like an exponential function with the time constant

$$t' = \left(\frac{b}{\pi \kappa} \right)^2 \quad (37)$$

Expressed in physical terms, this function determines the flow of heat from the initial heat source directly through the thickness of the plate. The time constant (37) can therefore be expected to be quite small for plates of ordinary thickness such as are used in the construction of aircraft.

For an aluminum plate,

$$\text{Thermal conductivity} = k = 0.504 \text{ cal}/(\text{cm})(\text{sec})(^\circ\text{C})$$

$$\text{Specific heat} = c = 0.217 \text{ cal}/(\text{g})(^\circ\text{C})$$

$$\text{Density} = \rho = 2.70 \text{ g}/\text{cm}^3$$

From this information, the thermal diffusivity is

$$\kappa^2 = \frac{k}{c\rho} = 0.086 \text{ cm}^2/\text{sec}$$

$$\kappa = \sqrt{0.086} = 0.93 \text{ cm}/\sqrt{\text{sec}}$$

Taking $b = 1/8$ inch = 0.318 centimeter, the time constant is

$$t' = \left(\frac{0.318}{0.93\pi} \right)^2 = 0.0119 \text{ sec} \quad (38)$$

The rise time of the temperature on the inner surface of the plate, directly opposite the heat source, should thus be of the order of 12 milliseconds. This result will not be particularly sensitive to the size of the initial heat source; that is, it does not depend greatly on the value of β , since the expression (37) for t' does not involve this parameter.

The temperature at the point 0 should have a maximum value, which is about

$$T_{0,\max} = \frac{Q}{c\rho\alpha^2 b} = \theta \frac{\beta}{b} \quad (39)$$

The initial rise of the temperature at the point 0 is determined by the flow of heat through the thickness of the plate, but its ultimate decline is governed by the transverse flow of heat along the plate. This is expressed by the functions $\varphi(\alpha;x,t)$ and $\varphi(\alpha;y,t)$, which, of course, have the same functional form.

From the initial conditions, the following is expected at $t = 0$:

$$\varphi(\alpha;x,0) = \begin{cases} 0 & \text{if } |x| > \alpha/2 \\ 1 & \text{if } |x| < \alpha/2 \end{cases} \quad (40)$$

It is easy to show from equation (28) that this is the case, if it is noted from equation (30) that

$$\left. \begin{aligned} g(-\eta) &= -g(\eta) \\ g(\infty) &= 1 \end{aligned} \right\} \quad (41)$$

The function $\varphi(\alpha;x,t)$ is roughly exponential in form and decays comparatively slowly in relation to the initial rapid rise of temperature at the point 0. It is best shown in the form of graphs drawn for special cases.

The analysis has assumed that the initial heat source has a square cross section and a depth β . In practice one will have little or no control over the exact shape of the region in which a lightning stroke develops heat in the plate; and on the whole one will probably find a circular or roughly elliptical spot. For points near the center of the spot and points away from the spot by distances large compared with the radius of the spot, the exact shape of the spot will be immaterial. For an exactly circular spot the analysis can be made in polar coordinates. This analysis is discussed in a later section for completeness, but its use would require numerical work with Bessel functions, which was not considered justifiable in view of the uncertainties in the data.

Graphical Example

In order to show the nature of the heat flow in the plate, a particular case is presented in graphical form. Consider an aluminum plate with the following dimensions:

$$\text{Thickness} = b = 0.318 \text{ cm (1/8")}$$

$$\text{Source size} = \begin{cases} \alpha = 0.5 \text{ cm} \\ \beta = 0.159 \text{ cm (1/16")} \end{cases}$$

The source is then assumed to be 0.5 centimeter square and extends half-way through the plate. From the data given in the preceding section for aluminum, the temperature of the source, for a given heat input Q , is initially

$$\theta = 10.3 Q \quad (42)$$

where Q is expressed in joules, and θ is the temperature rise above room temperature in degrees centigrade.

Temperature at point O. - The temperature at the point O, which is on the inside of the plate just opposite the center of the source, is considered first. Making use of equation (33) gives

$$\begin{aligned} T_0 &= T_0(0,0;t) \\ &= \theta |\varphi(\alpha;0,t)|^2 \psi(b, \frac{b}{2}; 0, t) \end{aligned} \quad (43)$$

The function $\psi(b, b/2; 0, t)$, which determines the flow of heat through the thickness of the plate, is plotted in figure 26. It starts from zero and rises to 0.5, since the flow of heat directly through the plate would double the amount of heated metal and so would lower the temperature by a factor 0.5. This function is plotted on a universal time scale as a function of t/t' , where t' is defined by equation (37).

The function $\varphi(0.5; 0, t)$, which determines the flow of heat away from the point O along the plate, is plotted in figure 27. This graph starts at unity at $t = 0$ and diminishes comparatively slowly to zero.

The composite result, giving the temperature at the point O, is plotted as curve A in figure 28, which shows that the temperature at O rises to about $\theta/4$ as its maximum value in about 20 milliseconds and then falls rather steeply; in 1/10 second it is down to $\theta/10$. This point will obviously be the hottest on the inside of the plate, so that the rapidity with which it cools off will be an important criterion governing the firing of an explosive gas mixture that contacts the surface here.

Temperature at a neighboring point. - As an indication of the temperatures reached on the inside of the plate near the source point, the temperature-time curve has been plotted for a point 0.5 centimeter from the point 0. The curve is given as curve B of figure 28. The temperature at this point rises slowly to only about 25 percent of the maximum temperature at 0 and then falls slowly. The flow of heat along the aluminum plate is so rapid that only the points quite near the initial source are heated to any great extent.

Effect of Continuous Source

It has been assumed in the previous calculations that the heat source is established instantaneously at time $t = 0$ and that only the temperature distribution from this origin is significant. In practice, the application of the heat will not be so instantaneous, but the source may be applied for some time and may vary from instant to instant in magnitude. Once the problem of finding the temperature distribution from an instantaneous source has been solved, it is possible to write the method of finding it from a variable source, taking advantage of the linearity of the differential equation of heat conduction and of the boundary conditions.

First the notation in which the result has been expressed will be revised. Instead of using the particular instant $t = 0$ as the time of application of the source, this instant is indicated as t_1 . Also, suppose that the heat is supplied in an infinitesimal time interval dt_1 , such that $Q = q(t_1)dt_1$. Then, from equation (31) the temperature distribution following from this source at times $t > t_1$ would be given by the formula

$$T(x, y, z, t) = \frac{q(t_1)}{c\rho\alpha^2\beta} \phi(\alpha; x, t-t_1)\phi(\alpha; y, t-t_1)\psi(b, \beta; z, t-t_1)dt_1 \quad (44)$$

Clearly, to find the temperature distribution from a set of sources operating in the past it is necessary only to sum (integrate) expression (44) over all the sources that have been present. This yields the final formula:

$$T(x, y, z, t) = \frac{1}{c\rho\alpha^2\beta} \int_{-\infty}^t q(t_1)\phi(\alpha; x, t-t_1)\phi(\alpha; y, t-t_1)\psi(b, \beta; z, t-t_1)dt_1 \quad (45)$$

It is not practicable to evaluate this expression by actual integration if the source function $q(t_1)$ is very complex. The best method

of handling it is probably by numerical and graphical means, approximating the source function by a set of discrete sources.

Treatment of Infinite Plate in Cylindrical Coordinates

The mathematical analysis of the heat flow in a plate has been carried out entirely in terms of Cartesian coordinates in the earlier sections of this report. This has led to the use of a heat source in the form of a small rectangular parallelepiped. The reader may consider that it would be more sensible to use a heat source in the form of a small cylinder. This is certainly correct in principle, and the procedure used has been one of convenience only. In this section the analysis is carried through for cylindrical polar coordinates with a cylindrical shape for the source and solved in terms of Bessel functions.

Using the usual cylindrical polar coordinates, with origin at the point 0, the heat-conduction equation takes the form

$$\left[\lambda^2 \left(\frac{\partial^2}{\partial r^2} + \frac{1}{r} \frac{\partial}{\partial r} + \frac{\partial^2}{\partial z^2} \right) - \frac{\partial}{\partial t} \right] T = 0 \quad (46)$$

Only cylindrically symmetric solutions need be considered, so that the temperature depends only on the distance from the center of the plate and not on the angular position around the source.

First, particular solutions of the differential equation (46) are sought which obey the boundary conditions of the problem. Here an infinitely large plate is taken at the start, so that the boundary conditions reduce to the requirement that the solution be finite everywhere, and be single-valued. There is to be no flow of heat from the surfaces of the plate, so that $\partial T / \partial z = 0$ at $z = 0, b$.

Particular solutions satisfying these conditions are of the form

$$F(r) \cos \left[\left(\frac{n\pi}{b} \right) z \right] \exp \left[- \left(\frac{n\pi\lambda}{b} \right)^2 t \right] \exp (-\lambda^2 t) \quad (47)$$

where λ is an arbitrary real positive constant, and $F(r)$ is a solution of the differential equation

$$\left(\frac{d^2}{dr^2} + \frac{1}{r} \frac{d}{dr} + \lambda^2 \right) F(r) = 0 \quad (48)$$

The only solution of equation (48) that remains finite at $r = 0$ (for $\lambda \neq 0$) is

$$F(r) = \text{constant} \times J_0(\lambda r) \quad (49)$$

where J_0 is the Bessel function of first kind of order zero.

To satisfy the initial conditions these particular solutions are combined linearly. The members in the variable z must be summed over the non-negative integer $n = 0, 1, 2, \dots$, while the radial solutions must be integrated over the parameter λ . If the initial heat source is a small cylinder of radius a and depth β , into which an amount of heat Q is deposited at $t = 0$, the result is

$$T(r, z, t) = \frac{Q}{c\rho\pi a^2 \beta} \varphi(a; r, t) \psi(b, \beta; z, t) \quad (50)$$

with

$$\psi(b, \beta; z, t) = \frac{\beta}{b} \sum_{n=0}^{\infty} \frac{(-1)^n \cos \left[\left(\frac{n\pi}{b} \right) z \right] \sin \left(\frac{n\pi\beta}{b} \right)}{\frac{1}{2}(1 + \delta_{n,0}) \frac{n\pi\beta}{b}} \exp \left[- \left(\frac{n\pi\beta}{b} \right)^2 t \right] \quad (51)$$

which is identical with the function defined in equation (20). The function $\varphi(a; r, t)$ is of the form

$$\varphi(a; r, t) = \int_0^{\infty} g(\lambda) J_0(\lambda r) \exp(-\lambda^2 t) \lambda \, d\lambda \quad (52)$$

where $g(\lambda)$ must be determined from the initial conditions. Here the following is required:

$$\varphi(a; r, 0) = \begin{cases} 0 & \text{if } r > a \\ 1 & \text{if } r < a \end{cases} \quad (53)$$

If

$$\varphi(a; r, 0) = u(r) \quad (54)$$

Then, from equation (52),

$$u(r) = \int_0^{\infty} g(\lambda) J_0(\lambda r) \lambda \, d\lambda \quad (55)$$

The inversion of this integral equation for $g(\lambda)$ when the left side is a known function gives

$$g(\lambda) = \int_0^{\infty} u(r) J_0(\lambda r) r \, dr \quad (56)$$

Making use of the initial conditions (53) which define the function $u(r)$, in the present problem

$$g(\lambda) = \int_0^a J_0(\lambda r) r \, dr \quad (57)$$

This leads to the formula

$$\begin{aligned} \phi(a; r, t) &= \int_0^{\infty} \left[\int_0^a J_0(\lambda R) R \, dR \right] J_0(\lambda r) \exp(-\lambda^2 t) \lambda \, d\lambda \\ &= \int_0^a \left[\int_0^{\infty} J_0(\lambda R) J_0(\lambda r) \exp(-\lambda^2 t) \lambda \, d\lambda \right] R \, dR \end{aligned} \quad (58)$$

It would be possible to make use of these formulas for the calculation of the temperature distribution in the plate, but the work would be greater than by the earlier method, without significant increase in accuracy of the result.

REFERENCES

1. Stout, H. P., and Jones, E.: The Ignition of Gaseous Explosive Media by Hot Wires. Third Symposium on Combustion and Flame Phenomena, The Williams & Wilkins Co., 1949, pp. 329-336.
2. Peirce, B. O.: A Short Table of Integrals. Third ed., Ginn and Company, 1929.

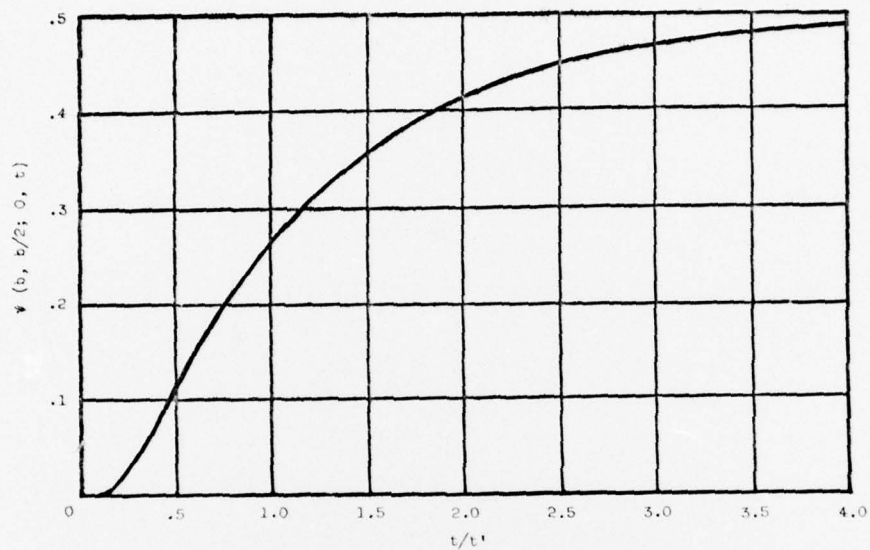


Figure 26. - Function $\psi(b, b/2; 0, t)$, which determines the flow of heat through the plate.

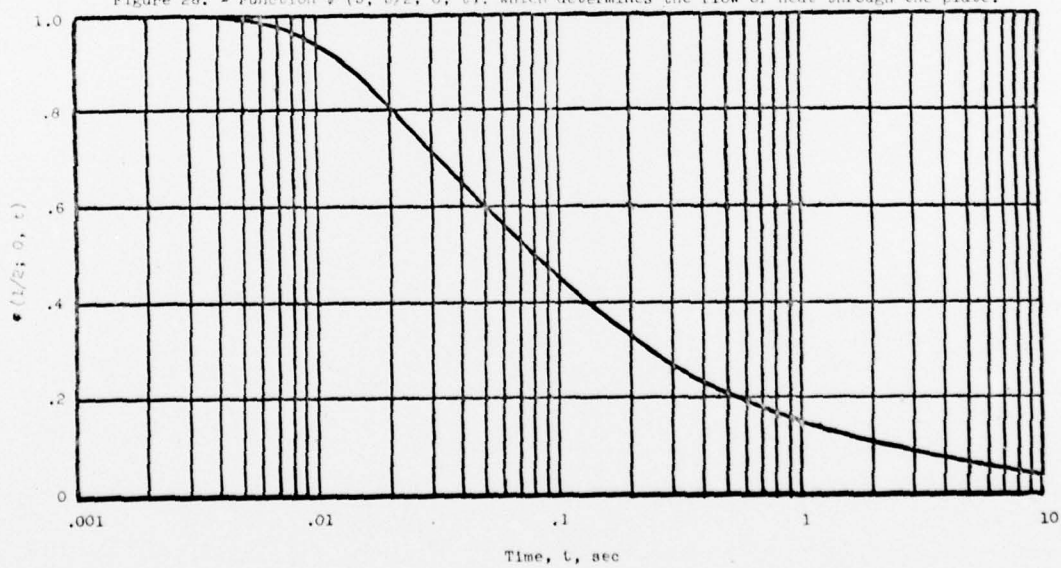


Figure 27. - Function $\psi(b, 1/2; 0, t)$, which determines the flow of heat along the plate.

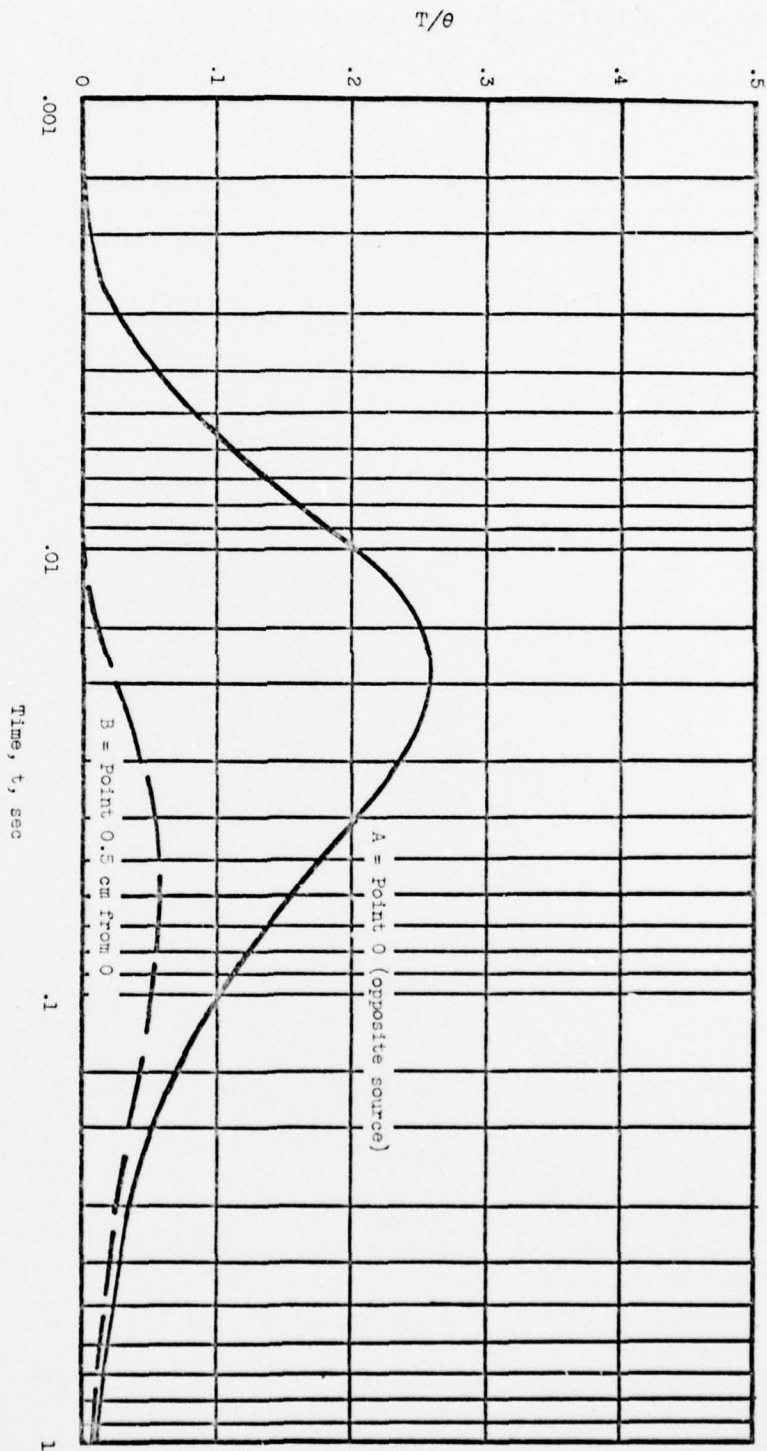


Figure 28. - Temperature-time curves; $b = 0.318$ centimeter ($1/8$ in.); $\beta = 0.159$ centimeter ($1/16$ in.); and $\alpha = 0.5$ centimeter.

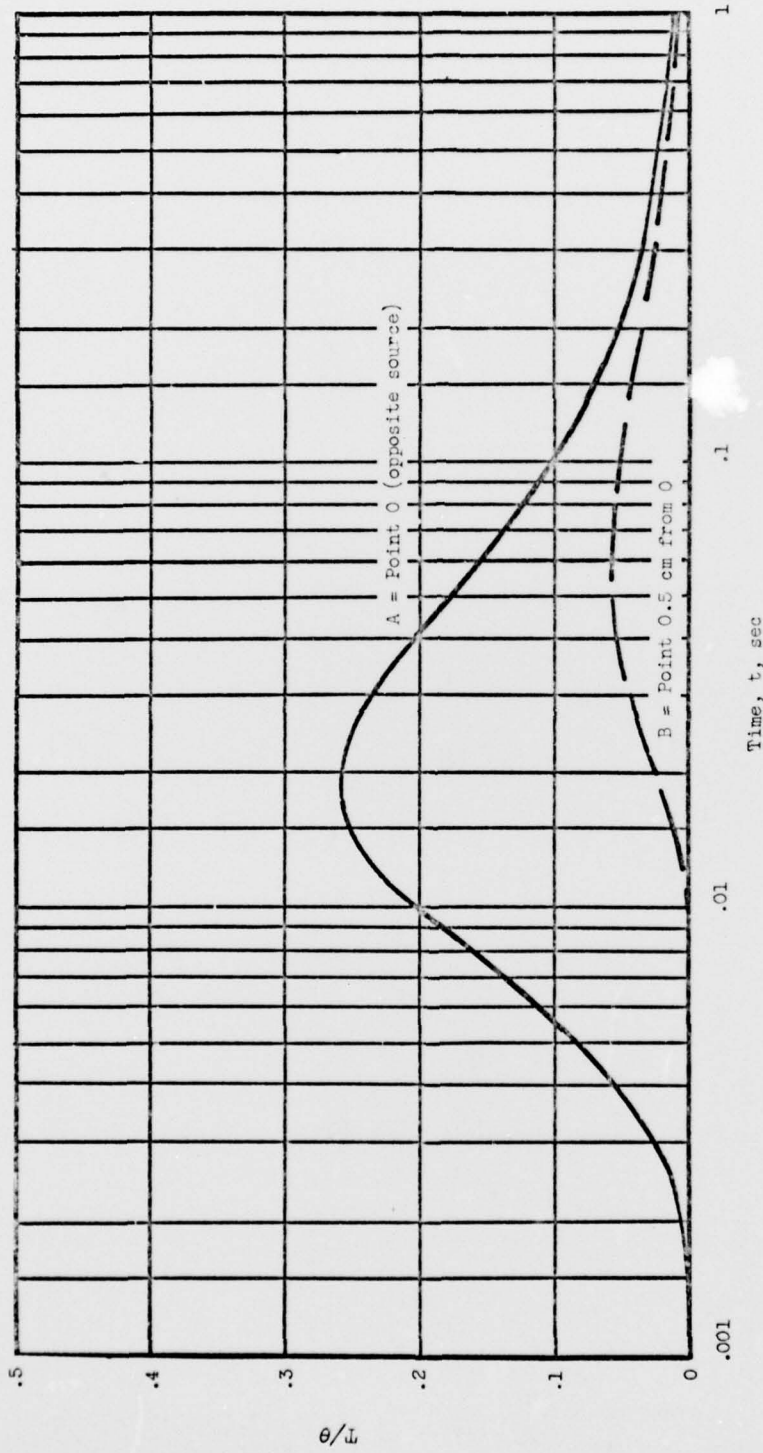


Figure 25. - Temperature-time curves; $b = 0.318$ centimeter ($1/8$ in.); $\beta = 0.159$ centimeter ($1/16$ in.); and $\alpha = 0.5$ centimeter.